

# Techno-economic and environmental impact assessment of a hybrid renewable energy system employing an enhanced combined dispatch strategy

Saheed Ayodeji Adetoro<sup>a,\*</sup>, Lanre Olatomiwa<sup>a,c,\*\*</sup>, Jacob Tsado<sup>a</sup>, Solomon Musa Dauda<sup>b</sup>

<sup>a</sup> Department of Electrical and Electronics Engineering, Federal University of Technology Minna, PMB 65, Minna, Nigeria

<sup>b</sup> Department of Agricultural and Bioresources Engineering, Federal University of Technology Minna, PMB 65, Minna, Nigeria

<sup>c</sup> Department of Electrical and Electronic Engineering Science, University of Johannesburg, 2006, Johannesburg, South Africa

## ARTICLE INFO

### Keywords:

HRES  
Dispatch strategies  
LCOE  
Sensitivity analysis  
Unreliable grid

## ABSTRACT

Developing countries face challenges in maintaining a reliable power supply due to factors such as ageing infrastructure and rapid urbanization. Relying on backup diesel generators during outages is not only ecologically hazardous but also economically inefficient. Integrating multiple renewable sources with conventional energy systems is crucial to meeting growing energy demands and reducing carbon emissions. This study assesses dispatch strategies for optimal operation in hybrid renewable energy systems (HRES) connected to an unreliable national grid (GRD). An enhanced combined dispatch (ECD) strategy is introduced for effective energy distribution, considering load demands, energy resource availability, and grid unreliability. Compared to load following (LF) and cycle charging (CC) strategies, the ECD strategy proves superior, resulting in an optimized HRES configuration with a 248 kW solar PV array, a 2 kW wind turbine (WDT), a 22 kW biogas generator (BGG), a 92 kW diesel generator (DiG), and a 658 kWh battery storage (BSS). Achieving a low Levelized Cost of Energy (LCOE) at 0.148 USD per kilowatt-hour and a Net Present Cost (NPC) of 1.99 million USD. Adopting the ECD strategy also exhibits substantial reductions in CO<sub>2</sub>, CO, SO<sub>2</sub>, and NO<sub>x</sub> emissions when compared to CC and LF. ECD achieves approximately 25% lower CO<sub>2</sub> emissions, 34% lower CO emissions, and a 40% reduction in SO<sub>2</sub> and NO<sub>x</sub> emissions. These findings highlight the ECD strategy's potential for effective, economically viable, and environmentally conscious energy solutions, particularly relevant in developing nations like Nigeria, where Hybrid Renewable Energy Systems could play a crucial role in the energy sector.

## 1. Introduction

Access to affordable and dependable energy is vital for both sustainable development and economic expansion. However, many developing countries, including Nigeria, face significant challenges in meeting their energy demands (Babatunde et al., 2019). Limited energy infrastructures, reliance on fossil fuels, and environmental concerns have necessitated the exploration of alternative energy sources, particularly renewable energy. Developing countries encounter various energy challenges, including inadequate access to electricity, overdependence on fossil fuels, high energy costs, and environmental degradation (Ugwoke et al., 2020). These issues hinder socio-economic development and exacerbate inequalities. Insufficient access to electricity restricts educational opportunities, healthcare services, and economic activities, perpetuating a cycle of poverty and underdevelopment.

Nigeria, the most populous country in Africa, faces severe energy challenges. Despite abundant energy resources, including oil and gas reserves, a large part of Nigeria's population lacks electricity access. In 2019, only 45% of Nigerians had electricity access, as reported by the International Energy Agency (IEA) (Remteng et al., 2021). This limited access hampers industrialization, job creation, and impedes overall economic growth (Azam et al., 2021). The newly elected president of Nigeria signed into law the Electricity Act of 2023, which supersedes the Electricity and Power Sector Reform Act of 2005 (NERC, 2005). The current law allows individuals to build, own, or operate electricity generation, especially from renewable energy sources, or distribution facilities without a license, provided that capacity limits are not exceeded. These limits include generating up to 1 MW of electricity in total at a location or distributing electricity with a total capacity of no more than 100 kW at a single site (PLAC, 2023).

\* Corresponding author.

\*\* Corresponding author.

E-mail addresses: [adetoroayo@fedpolybida.edu.ng](mailto:adetoroayo@fedpolybida.edu.ng) (S.A. Adetoro), [olatomiswa.l@futminna.edu.ng](mailto:olatomiswa.l@futminna.edu.ng) (L. Olatomiwa).

<https://doi.org/10.1016/j.gerr.2023.100044>

Received 14 September 2023; Received in revised form 1 December 2023; Accepted 2 December 2023

2949-7205/© 2023 The Author(s). Published by Elsevier B.V. on behalf of Shandong University. This is an open access article under the CC BY license (<http://creativecommons.org/licenses/by/4.0/>).

This change represents a positive stride in promoting renewable energy in Nigeria.

Hybrid renewable energy systems (HRES), combining various power sources like solar, wind, hydro, and biomass, have proven effective in addressing energy challenges in developing countries such as Nigeria (Olatomiwa et al., 2022; Olatomiwa et al., 2016). However, without an efficient dispatch strategy, the potential benefits of hybrid renewable energy systems may not be fully realized (Ramesh and Saini, 2020). Optimal dispatch strategy refers to the intelligent control and management of multiple energy sources in a hybrid system to ensure the most efficient and cost-effective allocation of energy. This approach optimizes energy generation, storage, and distribution, thereby enhancing system reliability, reducing operational costs, and maximizing the utilization of renewable resources (Lehtola and Zahedi, 2019; Olatomiwa et al., 2016a,b).

The dispatch approach for HRESs that incorporate battery backup but without diesel generators is simple: the battery charges when there is an excess of renewable energy compared to demand and discharges when the load exceeds the available renewable energy (Ishraque et al., 2022). However, in hybrid systems featuring both diesel generators and battery storage, dispatch strategies can become complex. The challenges mentioned involve deciding the primary power source for recharging a battery bank and determining whether to prioritize batteries or a diesel generator when renewable energy sources cannot meet energy demand (Adetoro et al., 2022a,b; Khiareddine et al., 2018).

Several studies have been conducted on the optimal sizing and planning of HRESs by employing various energy dispatch strategies. In the study conducted by Diyoke et al. (2023), the authors investigated the techno-environmental and economic performance of integrating optimal hybrid renewable power systems into an existing unreliable grid or using an off-grid HRES for university buildings in Nigeria. Power sources such as wind turbines, solar photovoltaic, battery banks, diesel engine generators, and converters are considered using the LF dispatch strategy. It was concluded that both grid-connected and standalone HRES can reliably and sustainably meet the electric load demand. The choice between grid-connected and off-grid systems depends on specific needs and constraints. Integration of both systems could enhance Nigeria's power supply resilience. Future studies should include actual measured resource data and explore the feasibility of large-scale energy storage systems. Dash et al. (2023) conducted a thorough analysis of multiple energy dispatch approaches, including LF, CC, and generator order (GO), to evaluate the performance of various battery energy storage technologies and mechanical energy storage systems in terms of energy, economics,

and environmental factors. The study focuses on the feasibility of power generation using wind turbines, bio-diesel generators, and tidal plants in a microgrid on the Andaman and Nicobar Islands in India. The results demonstrate the superiority of lithium-ion batteries (LIB) over lead-acid batteries and mechanical storage systems. The study determined that among various energy storage devices, a combination of wind, bio-diesel, tidal, and LIB with the cycle charging strategy exhibits the lowest NPC and cost of energy (COE). Various techno-economic indicators and sensitivity analyses are also considered.

Li et al. (2022) focused on the potential for hybrid renewable energy generation in resource-rich regions of China. HOMER Pro software was used to optimize hybrid energy systems in a small village in Nanyang, Henan province, focusing on economic, technical, and environmental factors. The research analyses various dispatch strategies, including the LF, CC, and CD approaches. The study's conclusion highlights the effectiveness of the PV/wind/diesel generator/battery system when employing the combined dispatch strategy, showcasing its superior economic viability based on total NPC and COE. Additionally, the PV-wind turbine-battery system stands out as the most favourable option from both economic and environmental perspectives, notably reducing CO<sub>2</sub> emissions compared to a system reliant solely on a diesel generator. Jurado et al. (2020) also investigated an off-grid renewable hybrid system in southern Ecuador, considering LF, CC, and CD strategies. The system comprised photovoltaic energy, hydrokinetic turbines, batteries, and biomass gasifiers. Different types of biomass were examined for the optimal system configuration. The study assessed NPC, LCOE, and CO<sub>2</sub> emissions for various control strategies, revealing the trade-offs between system cost, biomass consumption, and emissions. Aziz et al. (2022) introduced a novel dispatch strategy using MATLAB Link in HOMER software to optimize an off-grid energy system in rural Iraq that combined solar panels, diesel generators, and batteries to provide reliable electricity for rural electrification. This strategy incorporated a 12-hour foresight for load and solar production, and the results demonstrated its superiority over the default CC strategy. Uwineza et al. (2021) also identified shortcomings in HOMER's native dispatch algorithms (CC and LF) and proposed a new dispatch algorithm to address these issues. Their algorithm aims to minimize the NPC by prioritizing the usage of fuel cells (FCs) over other components in the hybrid energy system (HES). The algorithm was implemented using the MATLAB Version 2021a Link feature in the HOMER software. Odou et al. (2020) carried out a technical and economic feasibility study of implementing a HRES to provide sustainable rural electrification in Fouay village, Benin. The study utilizes

**Table 1**

Summary of related works on HRES dispatch strategies.

Reference	Location	System configuration	Dispatch strategy	Grid connection	Performance parameter
Aziz et al. (2019)	Diyala, Iraq	SPV-DiG-BSS	L F, CC, and CD	No	NPC, COE
Oladigbolu et al. (2019)	North-west, Nigeria	SPV-WDT-DiG-GRD	L F	Yes	NPC, COE, CO <sub>2</sub> emission
Toopshekan et al. (2020)	Tehran, Iran	SPV-WDT-DiG-BSS	L F and CC	Yes	NPC, COE, Initial Cost, Renewable fraction (RF)
Arévalo and Jurado (2020)	Ecuador	SPV-WDT- HKT-DiG-BDS	L F, CC, and CD	No	NPC, COE, Excess energy
Ramesh and Saini (2020)	Karnataka (India)	SPV-WDT-Hydro-DiG-BSS	L F, CC, and CD	No	NPC, COE, cost of fuel
Amin et al. (2020)	Iran	SPV-WDT-DiG-BSS-Bio-diesel Gen	L F, CC, and GO	No	COE, NPC, RF, CO <sub>2</sub> emission, Excess energy
Ramesh et al. (2021)	Karnataka	SPV-Micro-Hydro-WDT-DiG-BSS	L F, CC, and CD	No	COE, NPC
Shezan et al. (2021)	Kangaroo Island, South Australia	SPV-WDT-DiG-BSS	L F, CC, CD, GO, and PDS	No	NPC, COE, CO <sub>2</sub> emission
Ishraque et al. (2021)	Bangladesh	SPV-WDT-DiG-BSS	L F, CC, CD, GO, and PDS	No	NPC, COE
Yousef et al. (2022)	Atbara, Sudan	SPV-DiG- flywheel-BSS	L F, CC, CD, and PDS	No	NPC, COE
Shezan et al. (2022)	Dhaka and Khulna in Bangladesh	SPV-WDT-DiG-BSS	L F, CC, CD, GO, and PDS	No	NPC, COE, CO <sub>2</sub> emission
Ishraque et al. (2022)	Maldives	SPV-WDT-DiG-BSS-GRD	L F, CC, CD, GO, and PDS	Yes	NPC, COE, CO <sub>2</sub> emission
Hossen et al. (2022)	Kuakata, Bangladesh	SPV-DiG-WDT-BSS	L F, CC, CD, and GO	No	NPC, COE, CO <sub>2</sub> emission
Chen et al. (2023)	Iran	SPV-WDT-DiG-HKT-BSS	L F and CC	No	NPC, COE
Bekele et al. (2023)	Adama, Ethiopia	SPV-WST-DiG-BSS-Fuel Cell	L F and CC	Yes	NPC, CO <sub>2</sub> emission
Present study	North-central, Nigeria	SPV-WDT-BGG-DiG-BSS-GRD	L F, CC, and ECD	Yes (unreliable)	NPC, COE, Excess energy, GHG emission

HOMER software for optimization, simulation, and sensitivity analysis. The optimization output of the study is divided into three categories: architecture, costs, and system variables. Depending on the configuration, the optimal control strategy can either be CC or LF. Among these conditions, the hybrid PV/DiG/BSS with load following as the dispatch strategy was determined to be the option with the least cost.

Table 1 in this paper offers a concise overview of studies focused on designing HRES and the dispatch strategies they employ. Among these strategies, LF and CC are widely recognized. They both aim to optimize the reliability of HRES but, differ in their approach to managing battery charging and discharging alongside a diesel generator. In both LF and CC dispatch strategies, the diesel generator only serves as a backup and it is activated only when the available renewable energy falls short of meeting the load demand. The LF control strategy achieves maximal utilization of renewable energy by allowing the battery to charge solely with excess power generated by renewable energy sources (RES). The LF control strategy is cost-effective in areas with ample renewable energy potential but may lead to inefficient diesel generator use and higher greenhouse gas emissions during periods of low net load. In contrast, the CC strategy is suitable for regions with limited renewable resources. It activates the diesel generator to address energy deficits and charge the battery, thereby reducing the frequency of DiG activation. However, it may miss opportunities to store excess renewable energy if the battery is already charged by the diesel generator.

Additionally, the literature review reveals that the dispatch strategy commonly employed in the majority of grid-connected hybrid renewable energy systems (HRESs) involves relying on the grid as a reliable backup. This allows the grid to either supply additional energy during deficits or absorb excess energy when available (Bekele et al., 2023; Oladigbolu et al., 2019; Shezan et al., 2023). However, this operation creates significant challenges in developing nations like Nigeria, where the electrical grid is often unreliable. Also, there is no policy for selling surplus energy to the national grid.

Therefore, this study aims to combine the advantages of both LF and CC dispatch strategies by determining the optimum times to charge or not to charge the battery with DiG. Decisions will be made based on forecasts of future load demand and the expected energy generation from renewable energy resources. The proposed strategy's performance is evaluated in comparison to LC and CC strategies. The primary contributions of this study can be expressed as follows:

- Mathematical modelling of SPV, WDT, BGG, BSS, DiG and an unreliable grid power supply.

- Development of an adaptive dispatch strategy for HRES, considering grid unpredictability and renewable energy resource uncertainty.
- Comparative performance analysis of the proposed strategy with both LF and CC strategies.
- Techno-economic and environmental impact assessment of the HRES considering various dispatch strategies.

The rest of the paper is structured with the following sections: Section 2 discusses the case study and available energy resources, Section 3 details the mathematical models of system components, Section 4 addresses system optimization, and Section 5 presents and analyses the results. The paper concludes in Section 6.

## 2. Overview of the case study location

Maizube farm is the focal point of this study due to its significant potential for both biomass and solar energy resources. It is situated in the rural village of Sabon-daga, approximately 20 km from Minna, Niger state, Nigeria, with coordinates of  $9^{\circ} 25'36''$  N and  $6^{\circ} 22' 41''$  E. The farm covers an area of about 500 ha. The farm is organized into different units, including the Cowshed, Milking parlour, Feed processing centre, Milk processing unit, Administrative department, Orchard, and a school. It houses more than 100 dairy cows, capable of producing over 1000 L of milk daily. An aerial view of the farm centre can be seen in Fig. 1.

The farm's electricity usage is divided into four main activities: animal housing, feeding, milking, and milk refrigeration. The farm operates daily from 8:00 a.m. to 5:00 p.m., with milking taking place twice a day at 5:00 a.m. and 5:00 p.m., including Sundays and public holidays, lasting about an hour. The milk is rapidly cooled to  $4^{\circ}\text{C}$  within 4 h to maintain its purity. The farm's daily energy consumption averages 980 kWh, with an average load requirement of around 40 kW. Peak power usage reaches 82 kW, and the load factor is 0.49. The case study location experiences three distinct seasonal weathers: the dry season, which spans from February to April, followed by the rainy season from May to November, and finally, the Harmattan season in December and January, marked by cold and dry winds from the Sahara Desert. Energy consumption on the farm is elevated during the dry season because of the heightened utilization of air conditioners, fans, and water pumps to combat the effect of the heat. In contrast, energy consumption is relatively lower during the colder Harmattan season (Adetoro et al., 2023). Fig. 2 illustrates the daily load requirement for each season. The farm is connected to the national grid; however, the power supply is available only about 20% of the time (Adetoro et al., 2022a,b). To compensate for



Fig. 1. The aerial view of the case study location (Source: earth.google.com).

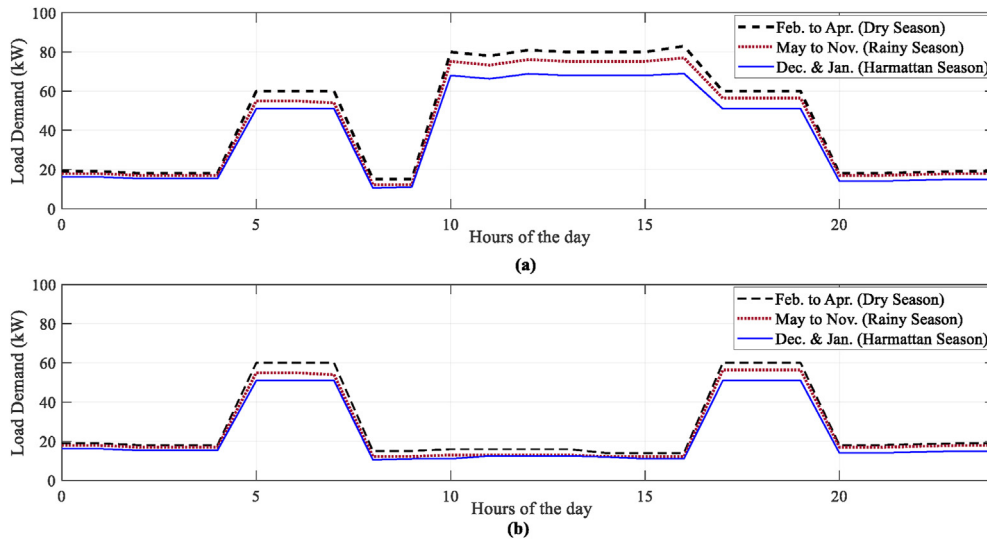


Fig. 2. Variations in the daily load demand at the Maizube farm centre for various seasons: (a) the average load profile at weekdays and (b) the average load profile at weekends (Adetoro et al., 2023).

grid power outages, standby diesel generators are used to meet the farm's energy demands (Adetoro et al., 2023).

2.1. Renewable energy resources available on-site

Nigeria's favourable geographic location places it within the global radiation belt, resulting in significant solar energy potential across its regions (Shaaban and Petinrin, 2014). This is notably true for the case study location, which experiences an average annual radiation of 5.49 kWh/m<sup>2</sup>/day. Seasonal variations are notable, with the lowest radiation in July of about 3.4 kWh/m<sup>2</sup>/day and the highest of around 6.926 kWh/m<sup>2</sup>/day in March. This highlights the attractiveness of solar energy as a power source for the study area. The performance of solar PV systems can be influenced to some extent by variations in operating temperature (Akhtari and Baneshi, 2019). The area maintains an average temperature of about 13°C, with January registering the lowest temperatures and March the highest. The hourly solar irradiance and temperature data for the specific study site were sourced from the solar energy surface meteorology database maintained by NASA (2016).

Data on wind speed for the location under study was unavailable; hence, wind speed data sourced from NASA's website (NASA, 2016) was also employed in this study. The average wind speed per month varies from 3.65 m/s in the month of July to 2.21 m/s in October. The annual average wind speed is 2.6 m/s, signifying a moderate potential for harnessing wind power.

The farm centre houses over 300 cows (foreign and local breeds), producing approximately 15 kg of manure per cow daily, creating a potential biogas resource of 4500 kg per day with minimal cost. The study proposes gathering organic waste from cow sheds to fuel a bio-digester. Biogas is produced from the organic waste through anaerobic digestion process. The produced biogas has the potential to serve as a fuel source for the generation of heat and/or electricity.

3. System component modelling

The schematic diagram in Fig. 3 depicts the proposed grid-connected HRES using a two-bus configuration. The AC and DC buses are interconnected through a bidirectional power converter. The system consists of various components, including solar photovoltaic (SPV), wind turbine

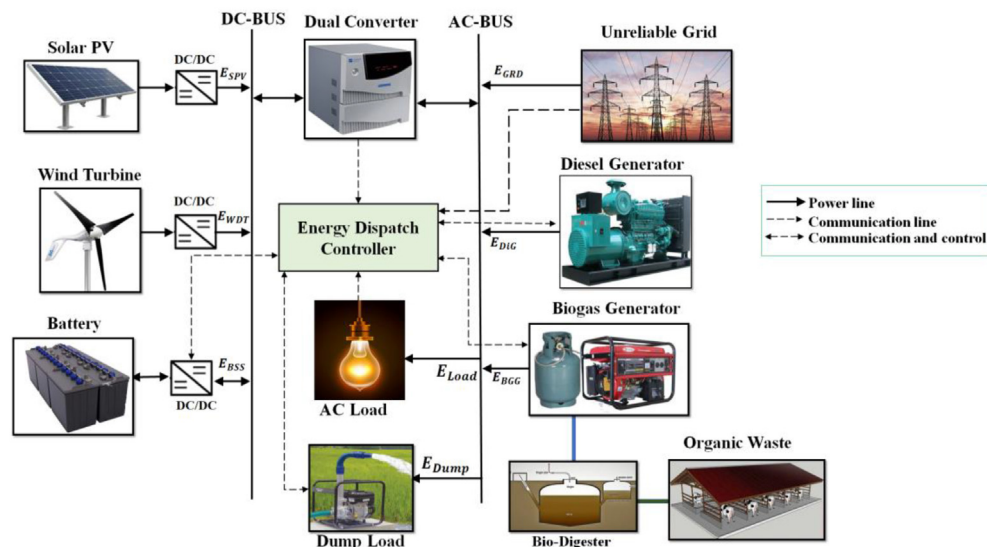


Fig. 3. Schematic of the proposed energy system configuration (Adetoro et al., 2023).

(WDT), power converters (CVT), utility grid (GRD), a battery storage system (BSS), biogas generator (BGG), and diesel generator (DiG). When all other sources have failed to meet a given period's load demand, DiG is then activated as a last option. The mathematical model of the suggested hybrid system configuration is shown in this section, so as to evaluate its performance. The economics and technical description of each of the system's component is presented in Table 2.

To formulate a system that is accurate and broadly applicable for characterizing various power flow scenarios, the study relies on the following assumptions:

- A time step interval of 1 h is considered in this study.
- The energy sources, as well as the electrical loads, are constant within each time step.
- Only the steady-state power and efficiency are taken into account.
- There are no perceptible changes to the system setup or plant capacity during the simulation.

### 3.1. Solar PV model

The two crucial input variables that can influence the power output of solar photovoltaic systems are solar irradiance and ambient temperature (Al-Subhi et al., 2020). The mathematical model utilized in the research to compute the solar PV's power output at time  $t$  ( $P_{SPV}(t)$ ) is based on a model in the reference (Akhtari and Baneshi, 2019; Mousavi et al., 2021).

$$P_{SPV}(t) = P_{SPV-r} \times d_{rf} \times \frac{G(t)}{G_{STC}} [1 + \alpha((T_{amb} + (0.0257 \times G(t))) - T_{STC})] \quad (1)$$

Where,  $P_{SPV-r}$  is the rated power (W) of the solar PV panel at standard test conditions (STC),  $d_{rf}$  represents the solar PV's derating factor,  $G(t)$  is the solar irradiance ( $W/m^2$ ) per hour,  $G_{STC}$  denotes the solar irradiance at STC,  $\alpha$  signifies the temperature coefficient of the SPV,  $T_{amb}$  represents the ambient temperature (C), and  $T_{STC}$  is the temperature at S T C (25C) of the solar PV.

### 3.2. Wind turbine model

Wind turbines are used to capture the energy of the wind to generate electrical power. The amount of power a wind turbine produces is primarily determined by the wind velocity. To account for variations in wind speed with altitude, it is often necessary to convert recorded wind speeds to the desired hub height of a wind turbine. This conversion is accomplished using the wind profile power law equation, represented by Eq. (2) (El-Sattar et al., 2021).

$$\mathcal{V}_{hub}(t) = \mathcal{V}_{ref}(t) \left( \frac{h_{hub}}{h_{ref}} \right)^\alpha \quad (2)$$

$\mathcal{V}_{hub}(t)$  represents the wind speed (m/s) at the WDT's hub height  $h_{hub}$  (m) and  $\mathcal{V}_{ref}(t)$  represents the reference wind velocity (m/s) measured at the anemometer height  $H_{ref}$  (m),  $\alpha$  denotes the friction coefficient. The hourly power output of the WDT ( $P_{WDT}(t)$ ) is estimated using Eq. (3) (Jamshidi et al., 2021).

$$P_{WDT}(t) = \begin{cases} 0 & \text{if } v_{hub} < v_{cut-in} \text{ OR } v_{hub} \geq v_{cut-out} \\ P_{WDT-r} \left( \frac{v_{hub}^3}{v_R^3 - v_{cut-in}^3} \right) - P_{WDT-r} \left( \frac{v_{cut-in}^3}{v_R^3 - v_{cut-in}^3} \right) & \text{if } v_{cut-in} \leq v_{hub} < v_R \\ P_{WDT-r} & \text{if } v_R \leq v_{hub}(t) < v_{cut-out} \end{cases} \quad (3)$$

$P_{WDT-r}$  (kW) is the WDT's rated power,  $\mathcal{V}_{hub}$  (m/s) denotes the wind speed at WDT's hub height,  $\mathcal{V}_r$  (m/s) is the rated wind speed of the WDT,  $\mathcal{V}_{cut-in}$  is the cut-in wind speed and  $\mathcal{V}_{cut-out}$  cut-out wind speed.

### 3.3. Battery bank model

Batteries storage can play a crucial role in HRES, as they store excess energy for usage when RESs are insufficient. The energy state of BSS at time  $t$  after the process of charging or discharging is expressed in Eqs. (4) and (5) respectively.

$$E_{BSS}(t) = E_{BSS}(t-1)(1 - \sigma) + E_{excess}\eta_{BSS} \quad (4)$$

$$E_{BSS}(t) = E_{BSS}(t-1)(1 - \sigma) - E_{deficit} \quad (5)$$

Where  $E_{BSS}(t-1)$  represent the energy state in the previous time step,  $\sigma$  is the self-discharge rate of the battery,  $E_{excess}$  is the excess energy stored in the BSS at time (t),  $\eta_{BSS}$  is the battery charging efficiency and  $E_{deficit}$  is the deficit energy supplied to the load at time (t).

The battery's mode at a given time  $t$  is primarily determined by its state of charge (SOC), refers to the current level of charge in a battery relative to its maximum capacity. SOC is the inverse of depth of discharge (DOD), meaning that  $SOC = 1 - DOD$ . The value of SOC can be determined using Eq. (10) as presented by Ajewole et al. (2022), and Atia and Yamada (2012).

$$SOC(t) = SOC(t-1) + \frac{\sum N_i P_i(t) - P_{load}(t)}{V_{BSS} C_{BSS}} \quad (6)$$

$N_i$  represents the number of generator units  $i$  and  $P_i$  denotes the power output of generator unit  $i$  at time  $t$ . The power generator indicator  $i$  is used to identify the specific generator unit.

Where  $i \in \{SPV, WDT, GRD, DiG, BGG\}$

### 3.4. Biogas generator model

The biogas generation system comprises a biodigester, biogas storage, and a biogas engine. This engine is linked to the gas pipeline and converts biogas from the biodigester's tank into electricity using an integrated generator, similar to a diesel engine. Biogas is used as fuel for combustion engines, which convert it into mechanical energy. This mechanical energy is then used to power an electric generator, generating electricity. Methane gas, which makes up 60%–70% of the entire volume of produced biogas, is its principal component; with trace amounts of oxygen, nitrogen, carbon dioxide, hydrogen sulphide, ammonia, hydrogen peroxide, and carbon monoxide (CO) also present (Malik et al., 2020).

To estimate the energy output from the BGG, the first step estimating the amount of biogas produced from the available biomass. This is done by considering a calorific value of biogas as 4700 kcal/m<sup>3</sup>, a conversion factor of 860, a gas generator with an electrical efficiency of 95%, and a combustion efficiency of 37% (Kasaeian et al., 2019). The water content of cattle manure is taken to be 78% and biogas yield is assumed to be 0.18 m<sup>3</sup> kg of dry cow dung (Suresh et al., 2020).

Eqs. (7) and (8) from Kasaeian et al. (2019) are utilized in this process to determine the biogas yield ( $Y_{BioG}$ ) and energy produce ( $E_{BGG}$ ).

**Table 2**  
Economics and technical specification of various components of the proposed system.

<b>Solar PV</b>	
Capital cost	\$1500/kW
Replacement cost	\$1300/kW
O&M cost	\$6/year
Temperature coefficient	-0.381%/°C
Efficiency	20.5%
De-rating factor	89%
Lifetime	25 years
<b>Wind turbine</b>	
Power output type	DC
Rated capacity	10 kW
Hub height	24 m
Cut-in wind speed	3.5 m/s
Cut-out wind speed	25 m/s
Rated wind speed	10 m/s
Initial cost per unit	\$55000
Replacement cost	\$52000
O&M cost	\$52/year
Lifetime	20 years
<b>Battery</b>	
Type	Lead-Acid
Rating	12 V, 84 Ah, 1 kWh
Initial cost per unit	\$300
O&M cost	\$5/year
Replacement cost	\$250
Self-discharge rate	0.15%/day
Depth of Discharge	30%
<b>Converter</b>	
Principal cost	\$300/kW
Replacement cost	\$250/kW
O&M cost	\$5/year
Lifetime	10 years
Inverter efficiency	95%
Rectifier efficiency	90%
<b>Grid</b>	
Grid Principal cost	\$0
Export tariff	\$0/kWh
Import tariff	\$0.07/kWh
Supply availability	20%
<b>Diesel generator</b>	
Initial cost per unit	\$195/kW
placement cost	\$190/kW
O&M cost	\$0.03/hour
Lifetime	15000 h
Maximum load ratio	25%
Diesel price	\$0.5/L
<b>Biogas generator</b>	
Rated capacity	5 kW
Calorific value of cow dung	860.4 Cal/kg
Conversion efficiency	25 %
Principal cost	\$600/kW
Replacement cost	\$600/kW
O&M cost	\$0.1/hr
Operation life	15000 h
<b>Control parameters</b>	
Project lifespan	25 years
Simulation time step	1 h
Annual capacity shortage	0%
Expected Inflation rate	20%
Interest rate	15%
Dispatch strategy	CC, LF and ECD

$$Y_{BioG} = 0.22M_{WDung} \times Y_{BioG}^{kg} \quad (7)$$

Where  $M_{WDung}$  represents the amount (in kilogram per year) of is wet cow waste and  $Y_{BioG}^{kg}$  is the biogas yield in cubic metres per kilogram of dry cow dung.

$$E_{BGG} = \frac{Y_{BioG} \times 1000 \times Cal_{BioG} \times \eta_{BGG}}{860} \quad (8)$$

Where,  $Cal_{BioG}$  denotes the calorific value (in  $kcal/m^3$ ) of biogas, and  $\eta_{BGG}$  is the total conversion efficiency of the BGG.

### 3.5. Diesel generator model

The primary requirement for distributed generation (DG) is to supply the entire net demand. The energy produced is determined by Eq. (9).

$$E_{DiG} = P_{DiG} \times \eta_{DiG} \times h_{opr} \quad (9)$$

Diesel generator fuel consumption is influenced by size and operational load, with optimum efficiency being attained between 80% and 100% of rated power. A diesel generator's fuel consumption (calculated in litres/kWh) can be determined using Eq. (10) (Gharibi and Askarza-deh, 2019).

$$F_c = AP_{DiG-O}(t) + BP_{DiG-L} \quad (10)$$

### 3.6. Power converter model

In a hybrid system that incorporates both alternating current (AC) and direct current (DC) power components, a bidirectional power converter is required to interconnect components. Specifically, a rectifier changes AC power to DC power, and an inverter converts DC power to AC power.

#### 3.6.1. Rectifier model

The rectifier plays a crucial role in converting AC power generated by the GRD, DiG, and BGG into a steady voltage DC power to charge the BSS. This conversion occurs during CC dispatch mode which is discussed in detail in section 4.1. The power supply to charge the BSS ( $P_{Rec-out}(t)$ ) can be estimated using Eq. (11).

$$P_{Rec-out}(t) = P_{Rec-in}(t) \times \eta_{Rec} \quad (11)$$

Where  $P_{Rec-in}(t)$  is the power supply to the rectifier from the AC source and  $\eta_{Rec}$  is the power rectifier's efficiency.

#### 3.6.2. Inverter model

The SPV, WDT and BSS in a hybrid energy system supplies DC power. To supply an AC load, a DC-to-AC conversion is necessary. The power supply to AC loads from DC sources ( $P_{Inv-out}(t)$ ) can be determined using Eq. (12).

$$P_{Inv-out}(t) = P_{Inv-in}(t) \times \eta_{Inv} \quad (12)$$

Where  $P_{Inv-in}(t)$  is the power supply to the inverter from the DC source to the rectifier  $\eta_{Inv}$  represents the power inverter's efficiency.

## 4. Hybrid energy system optimization

The optimization problem formulation involves the process of reliability and cost evaluation of the proposed HRES. It focuses on determining the optimal capacities of SPV, WDT, BSS, DIG, and BGG. This section covers the proposed energy dispatch strategy, system reliability, objective function, constraints, and a brief description of the algorithm adopted.

### 4.1. Proposed enhanced combined dispatch strategy

The dispatch strategy involves rules for managing generator and storage unit operations when renewable resources are insufficient for load demand. The proposed dispatch strategy aims to fuse the benefits of LF and CC dispatch strategies to optimize the benefit of renewable energy sources. This strategy involves making charging decisions for the battery, considering forecasts of future load demand and expected energy generation from

renewable resources. In each time step, the algorithm calculates the total renewable energy output and the load demand. The netload is determined by subtracting the aggregated renewable energy from the hourly load demand as expressed in Eq. (13). During each of the 8760 hourly time steps, the netload can either be a negative, zero, or positive value. Accordingly, various approaches are implemented to effectively manage energy under all conceivable scenarios. The diesel generator is employed as a last resort, typically during grid outages or when the biogas generator's energy output is insufficient to meet the demand. The processes of these operations are presented in Fig. 4(a)–(c) and discussed as follows:

$$P_{Net}(t) = P_{Load}(t) - \eta_{Inv}[P_{SPV}(t) + P_{WDT}(t)] \quad (13)$$

i. **Scenario 1** [ $\eta_{Inv}[P_{SPV}(t) + P_{WDT}(t)] = P_{Load}(t)$ ]: When the total renewable energy output matches the load demand, resulting in a netload of zero, the algorithm exactly meets the load demand without any surplus or deficit.

$$P_{Load} = \eta_{Inv}[P_{SPV}(t) + P_{WDT}(t)] \quad (14)$$

ii. **Scenario 2** [ $\eta_{Inv}[P_{SPV}(t) + P_{WDT}(t)] > P_{Load}(t)$ , and  $SOC = 100\%$ ]: If the total renewable energy output exceeds the load demand (net load is negative) and the battery SOC is at its maximum. The excess energy is supplied to the dump load. This is because there is no capability to feed excess energy back into the grid in the studied location.

$$P_{Load} = \eta_{Inv}[P_{SPV}(t) + P_{WDT}(t)] - P_{dump} \quad (15)$$

iii. **Scenario 3** [ $\eta_{Inv}[P_{SPV}(t) + P_{WDT}(t)] > P_{Load}(t)$ , and  $SOC < 100\%$  ]: In the case where the total renewable energy output exceeds the load

demand and the battery SOC is not at its maximum capacity. The battery storage is used to absorb the excess energy.

$$P_{Load} = \eta_{Inv}[P_{SPV}(t) + P_{WDT}(t)] - \frac{P_{BSS}}{\eta_{Rec}} \quad (16)$$

iv. **Scenario 4** [ $\eta_{Inv}[P_{SPV}(t) + P_{WDT}(t)] < P_{Load}(t)$ , and  $SOC > 30\%$ ]: If the total renewable energy output is insufficient to meet the load demand (net load is positive) and the battery SOC is not at its prescribed minimum threshold. The energy deficit is supplied to the battery bank.

$$P_{Load} = \eta_{Inv}[P_{SPV}(t) + P_{WDT}(t)] + P_{BSS}(t) \quad (17)$$

v. **Scenario 5** [ $\eta_{Inv}[P_{SPV}(t) + P_{WDT}(t)] < P_{Load}(t)$ ,  $SOC \leq 30\%$ , and  $\sum_t^{t+6} P_{Load}(t) - \sum_t^{t+6} P_{RE}(t) < 0$ ]: In scenarios where the cumulative renewable energy output is insufficient to satisfy the load demand, the battery SOC is at its minimum level, and the load demand forecast value is net-negative—signifying an upcoming surplus—the algorithm transitions to LF dispatch mode. In Load Following strategy mode (as described in Fig. 4(b)), the grid, biogas generator, or diesel generator supplies the net load alone and does not charge the battery bank. Instead, the battery storage is reserved to harness the anticipated excess energy generated by renewable sources. These described relationships are illustrated by Eqs. (18)–(20).

$$P_{Load} = \eta_{Inv}[P_{SPV}(t) + P_{WDT}(t)] + P_{GRD} \quad (18)$$

$$P_{Load} = \eta_{Inv}[P_{SPV}(t) + P_{WDT}(t)] + P_{BGG} \quad (19)$$

$$P_{Load} = \eta_{Inv}[P_{SPV}(t) + P_{WDT}(t)] + P_{DiG} \quad (20)$$

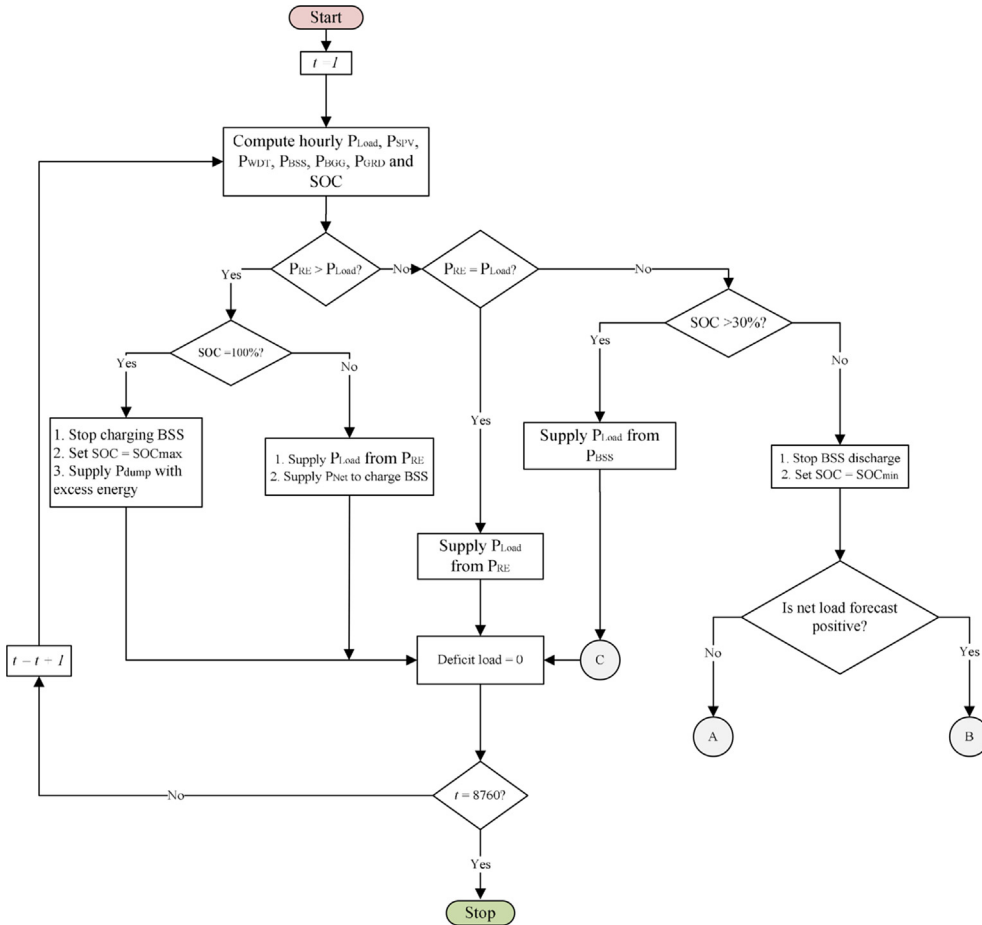


Fig. 4. (a) The main flowchart of the proposed ECD strategy for HRES coupled with an unpredictable grid. (b) Flowchart for The LF strategy operation. (c) Flowchart for The CC strategy operation.

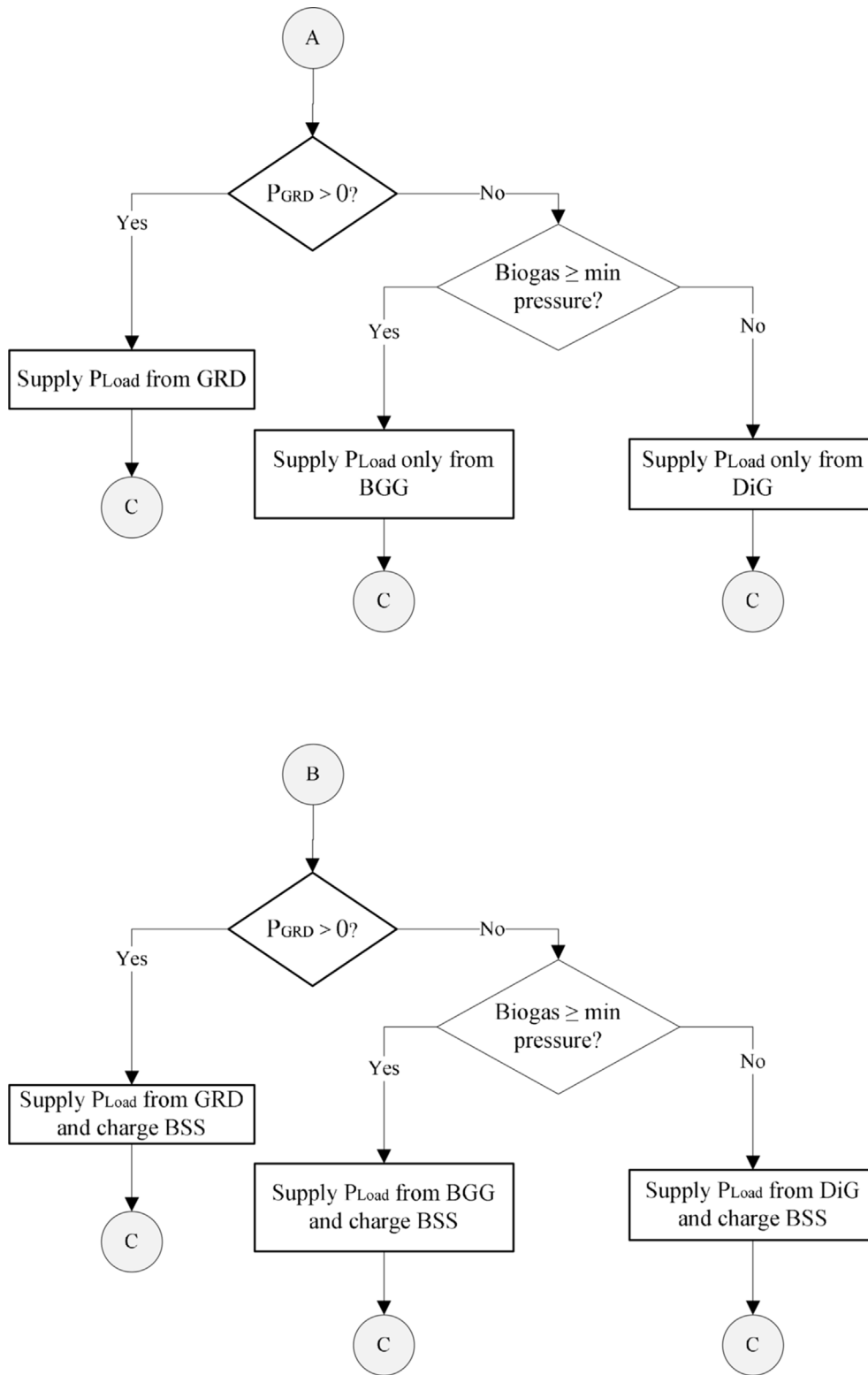


Fig. 4. (continued).

vi. **Scenario 6** [ $\eta_{Inv}[P_{SPV}(t) + P_{WDT}(t)] < P_{Load}(t)$ ,  $SOC \leq 30\%$ , and  $\sum_t^{t+6} P_{Load}(t) - \sum_t^{t+6} P_{RE}(t) \geq 0$ ]: If the total renewable energy output is not enough to meet the load demand, the battery SOC is at its minimum point and the load demand forecast indicates a net-positive value, signifying a projected energy deficit, the algorithm switches to

operate in CC dispatch mode. In CC strategy mode (as indicated in Fig. 4(b)), the grid, biogas generator, or diesel generator, prioritized in that sequence is used to supply the net load alone and charge the battery bank simultaneously. This approach ensures that the battery bank stores adequate energy to cover the predicted energy shortfall,

thereby averting the necessity of activating the diesel generator. The interrelationships between these components are mathematically described by Eqs. (21)–(23).

$$P_{Load} = \eta_{Inv}[P_{SPV}(t) + P_{WDT}(t)] + P_{GRD} - \frac{P_{BSS}}{\eta_{Rec}} \quad (21)$$

$$P_{Load} = \eta_{Inv}[P_{SPV}(t) + P_{WDT}(t)] + P_{BGG} - \frac{P_{BSS}}{\eta_{Rec}} \quad (22)$$

$$P_{Load} = \eta_{Inv}[P_{SPV}(t) + P_{WDT}(t)] + P_{DiG} - \frac{P_{BSS}}{\eta_{Rec}} \quad (23)$$

#### 4.2. Optimization technique

The study utilizes the Particle Swarm Optimization (PSO) technique due to its effective performance in identifying global optima, particularly suited for intricate problems (Adetoro et al., 2023; Amer et al., 2013; Mohamed et al., 2016). PSO is inspired by the collective behaviour of naturally swarming organisms like birds or fish. Initially, a population of particles is created with random location and velocity vectors. The fitness of each particle is determined based on its current location, and this fitness value is compared to its previous best performance.

By comparing the personal best fitness values of particles, a global best value is identified. If a particle's current position leads to a better fitness value than its previous best, its value is updated accordingly. Otherwise, it remains unchanged. The position of a particle is updated based on its velocity. The equation for updating the position of a particle is as follows:

$$X_i^{t+1} = X_i^t + V_i^{t+1} \quad (24)$$

Where  $X_i^{t+1}$  represents the particle's position in the next iteration,  $X_i^t$  is the current position of particle ( $i$ ) at iteration  $t$ , and  $V_i^{t+1}$  is the velocity for the next iteration.

The particle's velocity is adjusted using information from the best global particle (Gbest) and its personal best (Pbest) in each iteration as expressed in Eq. (25).

$$V_i^{t+1} = \omega V_i^t + c_1 r_1 (P_i^t - X_i^t) + c_2 r_2 (G^t - X_i^t) \quad (25)$$

Where,  $\omega$  is the inertia weight,  $c_1$  and  $c_2$  are acceleration factors for the cognitive and social components,  $r_1$  and  $r_2$  are random numbers between 0 and 1, for maintaining the population's diversity (Amer et al., 2013). The optimal sizing process using PSO techniques is depicted in Fig. 6. The overall process involves particles moving towards the optimal solution through iterations, and the best global solution continually updates. The dynamics of particles' movement in PSO can be visualized using a vector diagram as shown in Fig. 5.

#### 4.3. Objective function model

The objective function is the minimization of the Levelized Cost of Energy (LCOE). The objective is to determine the optimal component sizes of the HRES that will reliably satisfy the energy requirements of the studied location at the lowest possible cost. LCOE is the cost per kWh of energy produced by the system on average during its productive lifespan. The objective function is presented in Eq. (26).

$$\text{Minimise: } LCOE (\$/kWh) = \frac{(\sum N_j C_j) + P_{GRD} C_{GRD}}{\sum_1^{8760} P_{load}(t) / T_{SYS}} \quad (26)$$

$N_j$  is the number of component  $j$ . The annualized cost of a unit of component  $j$  is denoted by  $C_j$ ,  $P_{GRD}$  denotes the amount of annual energy supplied from the grid (kWh/yr),  $C_{GRD}$  is the price of electricity from the grid in \$/kWh and  $T_{SYS}$  is the lifecycle of the HRES.

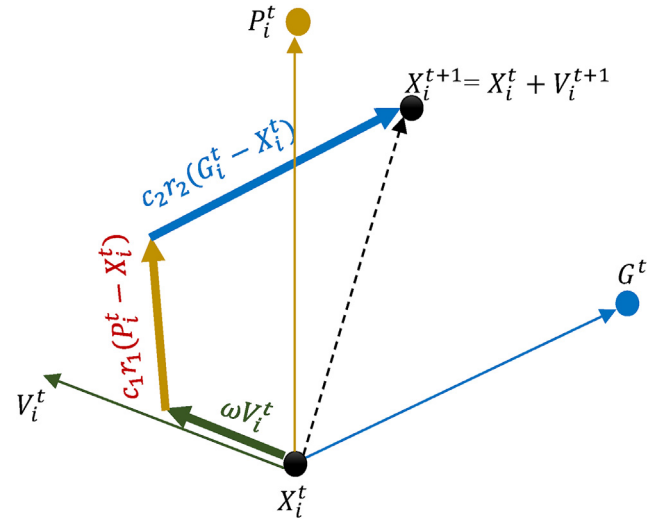


Fig. 5. Vector diagram of the movement of particles in PSO towards the optimal solution.

$$C_j = C_j^{A-CAP} + C_j^{A-O\&M} + C_j^{A-REP} - C_j^{A-SLV} \quad (27)$$

The total cost of each system component ( $C_j$ ) encompasses annualized capital costs ( $C_j^{A-CAP}$ ), annualized O&M cost ( $C_j^{A-O\&M}$ ), annualized replacement costs ( $C_j^{A-REP}$ ), and salvage value ( $C_j^{A-SLV}$ ).

##### 4.3.1. Annualize capital cost model

Annualized capital cost distributes the initial investment cost of the HRES across the system's expected operational life on an annual basis. The annualized capital cost for each system component is found using the Capacity Recovery Factor (CRF) as a coefficient in the calculation of the equivalent annual cost as expressed in Eq. (28).

$$C_j^{A-CAP} = CRF \times C_j^{CAP} \quad (28)$$

Where  $C_j^{CAP}$  is the initial capital cost of system component  $j$ .

CRF can be calculated based on component lifespan ( $L_j$ ) in years and the interest rate,  $i$  as shown in Eq. (29).

$$CRF = \frac{i(1+i)^{L_j}}{(1+i)^{L_j} - 1} \quad (29)$$

##### 4.3.2. Annualize operation and maintenance cost model

The total operation and maintenance cost (O&M) of component  $j$  ( $C_j^{A-O\&M}$ ) includes labour costs as well as the cost of consumables required to keep the component in operation.

$$C_j^{A-O\&M} = h_j C_j^{O\&M/h} \times CRF \quad (30)$$

Where  $h_j$  refers to the total operational hours of component  $j$  over its entire lifespan and  $C_j^{O\&M/h}$  is the hourly O&M cost of component  $j$ .

##### 4.3.3. Replacement cost model

The replacement of the HRES's component is required when the project's lifespan surpasses that of its components. The replacement cost involves cost of replacing or upgrading components due to wear or end of the component's life. The annualized replacement cost,  $C_j^{A-REP}$ , over the system's duration can be stated as:

$$C_j^{A-REP} = C_j^{REP} \times CRF \times \frac{1}{(1+i)^{L_j}} \quad (31)$$

where  $C_j^{REP}$  represents the replacement cost of component ( $j$ ).

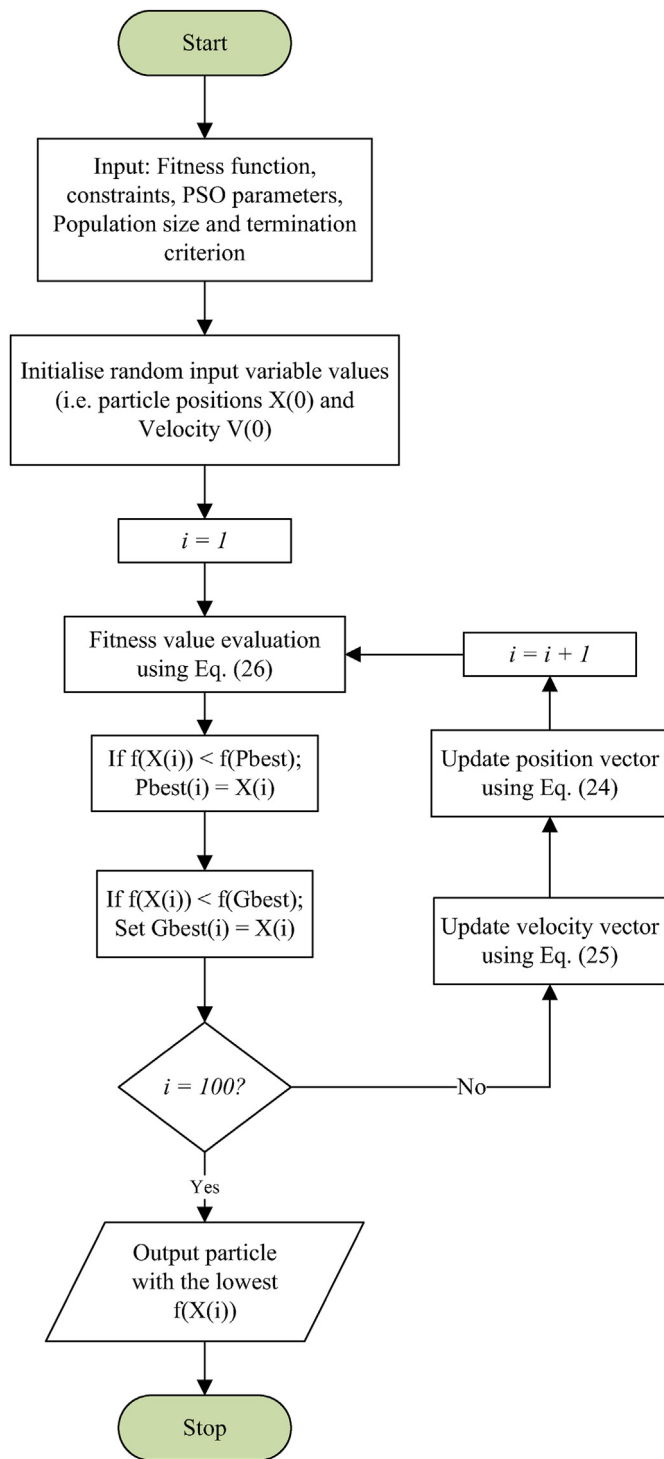


Fig. 6. Flowchart for optimal HRES component sizing using PSO technique.

4.3.4. Salvage value model

Salvage value is the estimated worth of a renewable energy system component at the end of its useful life. It is typically calculated as a fraction of the original purchase price and takes into account the remaining useful life as shown in Eq. (32).

$$C_j^{A-SLV} = C_j^{CAP} \frac{L_j^{Rem}}{L_j} \times \frac{1}{(1+i)^{L_j}} CRF \quad (32)$$

Where,  $L_j^{Rem}$  represent the remaining lifespan (in years) of component (j)

at the end of the system life and  $L_j$  is the total operational lifespan (in years) of component (j).  $C_j^{ASLV}$  is a cash inflow hence it is subtracted from the total system cost as outlined in Eq. (27).

4.3.5. Grid supply cost model

In addition to the costs associated with system components, the cost of power supplied from the utility grid is a critical economic factor to consider in grid-connected systems. Due to Nigerian policy restrictions, the proposed HRES is designed to solely supply energy from the grid and not feed energy to the grid. Grid energy supply cost ( $C_{GRD}$ ) represents the average annual cost of energy obtained from the national grid throughout the HRES's operational life and can be expressed as in Eq. (33).

$$C_{GD} = C_{GD}^{kWh} \times \sum_0^{8760} P_{GRD}(t) \quad (33)$$

Where,  $C_{GD}^{kWh}$  is the cost of energy unit (\$/kWh) supplied from the grid and  $P_{GRD}(t)$  is the amount of power supplied from the grid at hour  $t$ .

4.3.6. System constraints model

In this study, the energy system optimization process has to adhere to certain practical and technical limitations to produce feasible solutions. The primary constraint, defined in Eq. (34), relates to maintaining an energy balance between the power sources and the farm's energy demand consistently.

$$\sum N_j P_j(t) \geq P_{Load}(t) \quad (34)$$

Where  $P_j(t)$  denotes the amount of power output at time  $t$ , from each energy source  $j$ .

$$Decision\ variables = \begin{cases} 1 \leq N_{SPV} \leq 1500 \\ 1 \leq N_{WDT} \leq 200 \\ 1 \leq N_{BSS} \leq 1500 \\ 1 \leq N_{BGG} \leq 100 \\ 1 \leq N_{DiG} \leq 400 \end{cases} \quad (35)$$

Eq. (35) outlines the lower and upper limits for the variables. The third constraint specifies the permissible range for charging and discharging BSS, ensuring its longevity, as represented in Eq. (36).

$$SOC_{min} \leq SOC(t) \leq SOC_{max} \quad (36)$$

Table 3  
The optimal component sizes using LF, CC and ECD.

Component	Unit	CC dispatch strategy	LF dispatch strategy	ECD strategy
SPV	kW	235	255	248
WDT	kW	2	2	2
CVT	kW	119	95.2	100
BGG	kW	22	22	22
DiG	kW	92	65	92
BSS	kWh	885	647	658

Table 4  
Economic performance comparison of LF, CC and ECD.

Parameters	Unit	CC dispatch strategy	LF dispatch strategy	ECD strategy
NPC	\$	2.36 M	2.05 M	1.99 M
LCOE	\$/kWh	0.170	0.162	0.148
Simple payback period	year	6.90	6.10	5.28
Discounted payback period	year	3.93	3.90	3.91

5. Result and discussion

A comparative analysis was conducted to assess the effectiveness of three different strategies—LF, CC, and ECD—in optimizing the sizing of an Energy System using the PSO algorithm. The simulation was conducted in a MATLAB 2020a, focusing on the optimization of component sizes to achieve the lowest LCOE.

5.1. Economic comparison

Table 3 and Table 4 present the optimal component sizes and economic advantage obtained from employing various dispatch strategies to meet the total load demand of the specified location. The results

highlighted the superiority of the ECD strategy, yielding an optimal configuration with a 248 kW solar PV array, a 2 kW wind turbine, a 22 kW biogas generator, a 92 kW diesel generator, and 658 kWh battery storage, exhibiting the lowest LCOE and NPC values of 0.148 USD per kilowatt-hour and 1.99 million US dollars respectively. When comparing the optimized configuration with the existing setup that relies on a diesel generator and an unreliable grid power system at the case study farm centre, the simple payback period for the proposed system configuration is approximately 5 years and 3 months.

Figs. 9(a)–(c) and 10(a)–(c) provide a visual illustration of how the energy dispatch strategies are employed to meet load requirements on both typical weekdays and weekends in March. The Diesel Generator comes into play when the combined energy output from renewable

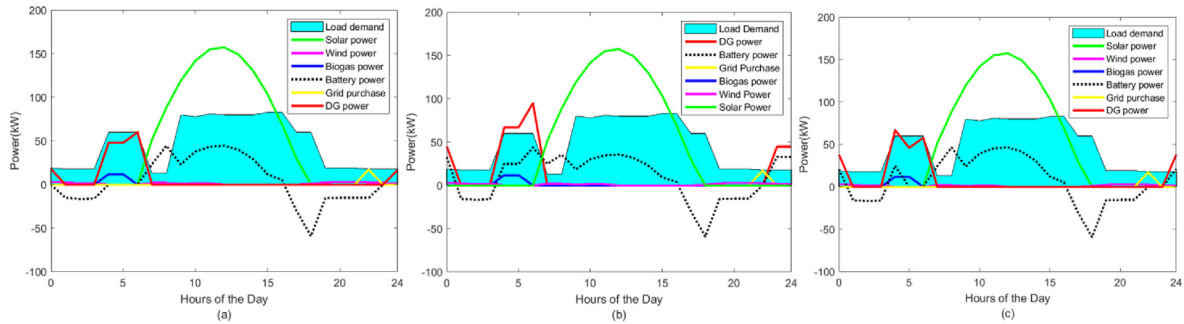


Fig. 7. Power contribution by various power sources to meet the load demand for the Third Monday in March adopting various energy dispatch strategies: (a) LF; (b) CC; (c) ECD.

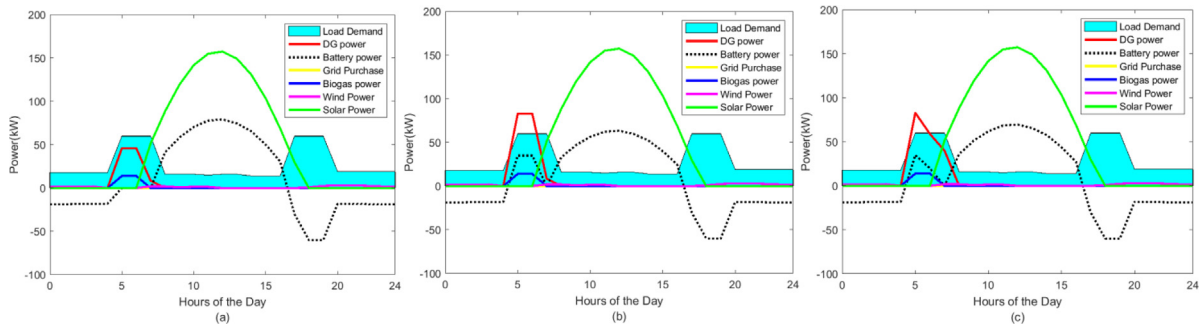


Fig. 8. Power contribution by various power sources to meet the load demand for the Third Sunday in March adopting various energy dispatch strategies: (a) LF; (b) CC; (c) ECD.

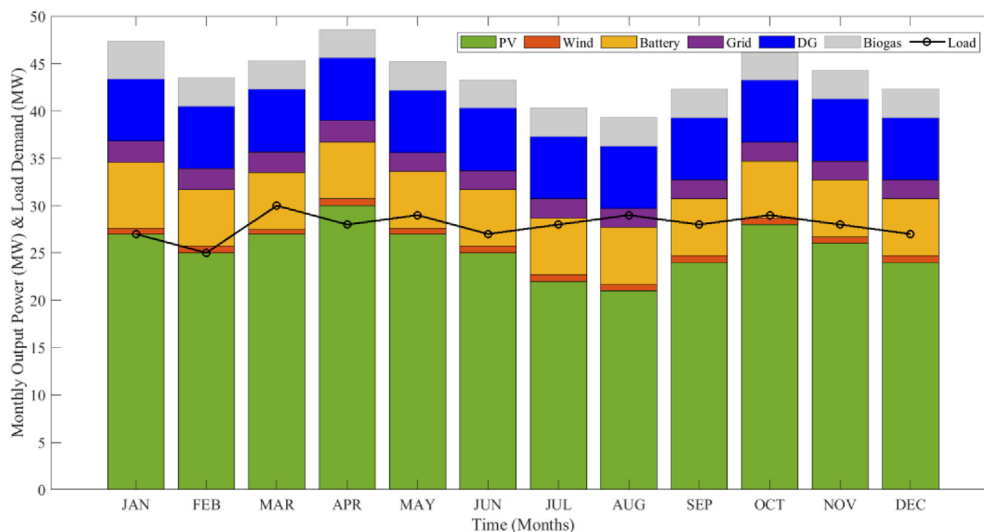


Fig. 9. Bar chart of the monthly energy production of different energy sources alongside the load demand.

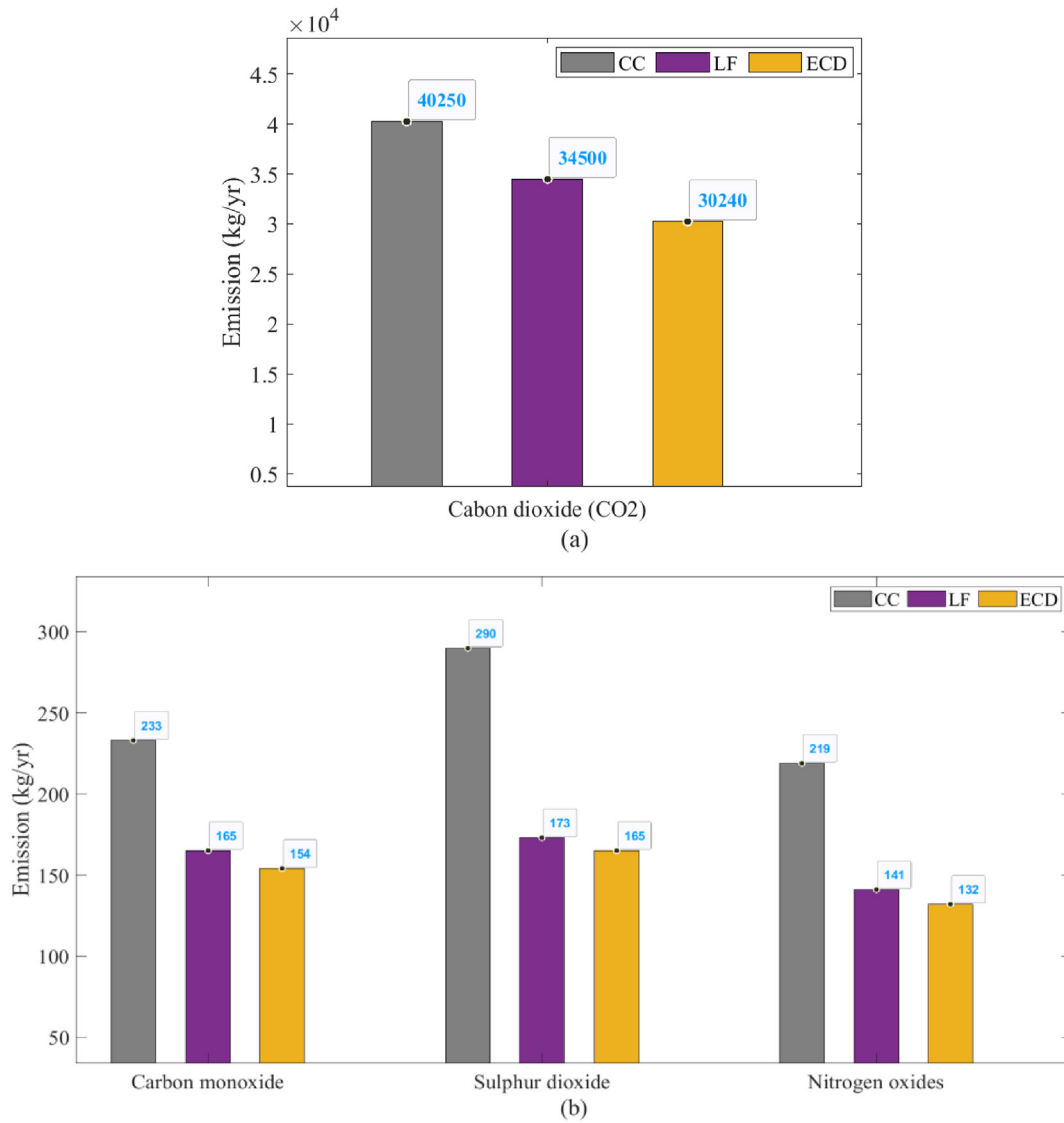


Fig. 10. GHGs emission comparison of LF, CC and ECD: (a) CO<sub>2</sub> emissions; (b) Other gases.

sources and batteries cannot meet the load demand, and there is no power supply from the grid. As discussed earlier under the LF operational approach, the DiG is activated exclusively to cater to the net load without simultaneously recharging the Battery Storage. Conversely, in the CC strategy, the DiG is employed both to fulfil the energy deficit and to charge the BSS concurrently. In the case of the ECD strategy, a smarter decision-making process comes into play. The system determines the best instances to switch between LF and CC strategies. In Figs. 7(c) and 8(c), for instance, at approximately 15:00hr, the projected netload value is

positive. As a result, the system operates in CC mode to address the deficit until around 4:00hr the following day, when the forecasted value turns negative. This negative value indicates an anticipated surplus of energy. Consequently, the system transitions to the LF dispatch strategy.

In Fig. 9, the monthly energy contributions from different system components to meet the load demand are depicted. The primary energy source is solar PV, making up approximately 68% of the annual energy output. In contrast, wind turbines contribute the least, accounting for less than 2% of the total energy generation. This distribution aligns with the

Table 5  
Performance comparison of LF, CC and ECD.

Parameter	Unit	LF dispatch strategy	CC dispatch strategy	ECD strategy
Renewable fraction	%	86.1	76.2	85.7
Renewable energy production	kWh/year	557192	513958	543334
DG production	kWh/year	5621	6868	6483
DG operating time	h/year	209	244	242
Fuel consumption	L/year	2354	2482	2085
Battery throughput	kWh/year	108999	101099	110004
Battery autonomy	h	13.60	9.98	10.01
Excess energy	kWh/year	140253	210742	146585
Percentage of excess energy	%	26.6	33.5	20.5

renewable energy resources available at the specific case study location. The overall renewable fraction of the system is 84.7%.

## 5.2. Technical performance comparison

Furthermore, Table 5 provides a comprehensive performance comparison of the three dispatch strategies. Since the peak demand period aligns with the period of maximum solar PV energy production, the analysis reveals that the LF strategy demonstrates a slightly higher penetration of renewable energy compared to ECD. However, ECD exhibits a lower level of fuel consumption in comparison to LF. The difference in fuel consumption can potentially be attributed to the fact that the DiG operates more efficiently within the context of the ECD strategy. The LF strategy presents the least excess energy production, followed closely by the ECD strategy. On the other hand, the CC strategy displays the least favourable performance with the highest LCOE, fuel consumption, and excess energy production.

## 5.3. Environmental performance comparison

Fossil fuel-based power generators may be essential to improve the reliability of HRES, especially during days of insufficient output from renewable energy sources and in regions with unreliable grid infrastructure. However, the combustion of fossil fuels in generators is a significant contributor to greenhouse gas (GHG) emissions, exacerbating climate change and its associated environmental and societal impacts. The environmental performance comparison among the dispatch strategies reveals notable differences in their emissions profiles. Fig. 10 illustrates the emissions of carbon dioxide (CO<sub>2</sub>), carbon monoxide (CO), sulphur dioxide (SO<sub>2</sub>), and nitrogen dioxide (NO<sub>x</sub>) resulting from the three dispatch strategies under discussion. It should be noted that NO<sub>x</sub> comprises a composite of both nitric oxide (NO) and nitrogen dioxide (NO<sub>2</sub>). When comparing the CC strategy to the ECD strategy, the differences in emissions are striking. Compared to the CC strategy, the adoption of the ECD strategy results in notable reductions in emissions. Specifically, when CO<sub>2</sub> emissions, CC generates 40250 kg per year, whereas ECD emits 30240 kg per year. This signifies a substantial reduction of approximately 25% in annual CO<sub>2</sub> emissions when ECD is employed. In the context of CO emissions, CC produces 233 kg per year, while ECD

emits a considerably lower 154 kg per year. This translates to a significant 34% reduction in annual CO emissions when ECD is adopted. Furthermore, both SO<sub>2</sub> and NO<sub>x</sub> emissions exhibit a substantial 40% reduction in annual emissions when transitioning from CC to ECD strategy.

Likewise, in the comparison between LF and ECD, ECD remains the stronger performer in terms of emissions reduction. LF results in annual CO<sub>2</sub> emissions of 34500 kg/year, representing a 14% reduction in annual CO<sub>2</sub> emissions in favour of ECD. In cases of CO, SO<sub>2</sub> and NO<sub>x</sub> emissions, the result shows 7%, 5% and 6% respectively. In both comparisons, the ECD strategy consistently demonstrates an adequate reduction in emissions compared to LF and CC. This modest reduction in GHG emission can make a significant difference when aggregated over the 25-year life cycle of the system. These comparisons indicate the superior environmental performance of the ECD strategy over LF and CC, with significantly lower emissions across all categories.

## 5.4. Sensitivity analysis

Sensitivity analysis plays a crucial role in assessing the robustness and viability of renewable energy systems in the face of changing input parameters. In this study, sensitivity analysis examines the impact of increasing fuel prices and inflation rate on the optimal size, cost and renewable energy penetration. From the result presented in Table 6 when diesel price increases from \$0.75 to \$1, the impact on the optimal system is relatively minor. However, with a further rise in fuel cost, there is a noticeable effect. For instance, the increase in diesel cost from \$0.75 to \$1.50 (a 100% rise) leads to a 103.8% rise in initial capital costs of the system and a 24.6% uptick in NPC. However, the fuel costs decreased by 60.5%. This reduction in fuel cost is due to higher diesel prices making diesel generators less cost-effective, prompting the use of more renewable sources to meet energy needs. As a consequence, there is an increased adoption of renewable energy, leading to an initial rise in capital costs while simultaneously lowering operational and fuel expenditures.

In contrast, according to the results presented in Table 7, changes in the inflation rate have a limited impact on the NPC. This is likely due to the fact that the initial cost is the major component of the renewable energy system cost. However, it is worth noting that as the inflation rate rises, there is a noticeable increase in both the O&M cost and the fuel cost since they are recurring costs.

**Table 6**  
Result analysis for changes in the diesel prices.

Inflation Rate (%)	Diesel Price (\$)	Solar PV (kW)	No. of Batt.	DG (kW)	BioGas Gen.	Converter (kW)	LCOE (\$/kWh)	NPC (\$)	Initial Cap. Cost (\$)	O&M Cost (\$/yr)	Fuel Cost (\$/yr)	Renew Fractn (%)	Discountd payback (yrs)
20	0.75	248	232	92	22	100	0.148	1.99 M	421148	15920	20564	84.7	3.91
20	1.00	269	864	92	22	102.5	0.167	2.05 M	567843	14417	16873	86.4	3.97
20	1.25	308	1452	92	25	105	0.176	2.12 M	758742	13815	14421	89.1	4.02
20	1.50	339	1580	92	25	105	0.193	2.16 M	943224	13371	12481	90.8	4.03
20	2.00	340	1584	92	25	112	0.198	2.20 M	953320	13022	12759	95.0	4.05

**Table 7**  
Result analysis for changes in the rate of inflation.

Inflation Rate (%)	Diesel Price (\$)	Solar PV (kW)	No. of Batt.	DG (kW)	BioGas Gen.	Converter (kW)	LCOE (\$/kWh)	NPC (\$)	Initial Cap. Cost (\$)	O&M Cost (\$/yr)	Fuel Cost (\$/yr)	Renew Fractn (%)	Discountd payback (yrs)
18	0.75	198	289	90	22	100	0.150	1.68 M	373544	16203	22745	78.1	4.06
19	0.75	215	278	90	22	100	0.149	1.79 M	379723	16160	21983	78.6	3.87
20	0.75	248	232	92	22	100	0.148	1.99 M	421148	15920	20564	84.7	3.91
21	0.75	269	221	92	25	95	0.131	2.23 M	450763	15889	20956	85.6	3.87
22	0.75	290	219	92	25	100	0.126	2.57 M	456991	15835	20792	85.7	3.71

## 6. Conclusion

In conclusion, the comprehensive study conducted a comparative analysis of three different strategies—LF, CC, and ECD—to optimize the sizing and operation of a HRES connected to an unreliable grid, aimed to minimize the LCOE by optimizing component sizes. The ECD strategy emerged as superior, achieving the lowest LCOE of 0.148 USD per kilowatt-hour and an NPC of 1.99 million USD. This superiority was confirmed by comparing with existing setups, showing a promising payback period of about 5 years and 3 months. The ECD strategy also demonstrates significant reductions in emissions compared to CC and LF strategies. In the CC vs. ECD scenario, CO<sub>2</sub> emissions decrease by 25%, while CO emissions decrease by 34%. Switching from LF to ECD yields a 14% decrease in CO<sub>2</sub> emissions, showing the superior environmental efficiency of the ECD approach. Performance assessments showcased the ECD strategy's adaptive ability between LF and CC modes for efficient energy distribution. These findings collectively emphasize the potential of the ECD strategy to offer effective, economically viable, and environmentally conscious energy solutions, particularly relevant in developing nations like Nigeria where Hybrid Renewable Energy Systems play a crucial role.

## Declaration of competing interest

The authors declare that they have no known competing financial interests or personal relationships that could have appeared to influence the work reported in this paper.

## References

- Abd El-Sattar, H., Kamel, S., Sultan, H., Tostado-Véliz, M., Eltamaly, A.M., Jurado, F., 2021. Performance analysis of a stand-alone pv/wt/biomass/bat system in alrashda village in Egypt. *Appl. Sci.* 11 (21). <https://doi.org/10.3390/app112110191>.
- Adetoro, A.S., Olatomiwa, L., Tsado, J., Dauda, S.M., 2023. e-Prime - advances in Electrical Engineering, Electronics and Energy A comparative analysis of the performance of multiple meta-heuristic algorithms in sizing hybrid energy systems connected to an unreliable grid. *E-Prime - Advances in Electrical Engineering, Electronics and Energy* 4 (February), 100140. <https://doi.org/10.1016/j.eprime.2023.100140>.
- Adetoro, S.A., Nwohu, M.N., Olatomiwa, L., 2022a. Techno-economic analysis of hybrid energy system connected to an unreliable grid: a case study of a rural community in Nigeria. In: 2022 IEEE Nigeria 4th International Conference on Disruptive Technologies for Sustainable Development (NIGERCON), pp. 1–5. <https://doi.org/10.1109/NIGERCON54645.2022.9803128>.
- Adetoro, S.A., Olatomiwa, L., Tsado, J., Dauda, S.M., 2022b. An overview of configurations and dispatch strategies in hybrid energy systems. In: 2022 IEEE Nigeria 4th International Conference on Disruptive Technologies for Sustainable Development (NIGERCON), pp. 10–15. <https://doi.org/10.1109/NIGERCON54645.2022.9803082>.
- Ajewole, T.O., Oladepo, O., Hassan, K.A., Olawuyi, A.A., Onarinde, O., 2022. Comparative study of the performances of three metaheuristic algorithms in sizing hybrid-source power system. *Turkish Journal of Electrical Power and Energy Systems* 10, 1–13. <https://doi.org/10.5152/tepes.2022.22012>.
- Akhtari, M.R., Baneshi, M., 2019. Techno-economic assessment and optimization of a hybrid renewable co-supply of electricity, heat and hydrogen system to enhance performance by recovering excess electricity for a large energy consumer. *Energy Convers. Manag.* 188 (January), 131–141. <https://doi.org/10.1016/j.enconman.2019.03.067>.
- Al-Subhi, A., El-Amin, I., Mosaad, M.I., 2020. Efficient predictive models for characterization of photovoltaic module performance. *Sustain. Energy Technol. Assessments* 38 (February), 100672. <https://doi.org/10.1016/j.seta.2020.100672>.
- Amer, M., Namaane, A., Sirdi, N.K.M., 2013. Optimization of hybrid renewable energy systems (HRES) using PSO for cost reduction. *Energy Proc.* 42, 318–327. <https://doi.org/10.1016/j.egypro.2013.11.032>.
- Amin, M., Rad, V., Shahsavari, A., Rajaei, F., Kasaean, A., 2020. Techno-economic assessment of a hybrid system for energy supply in the affected areas by natural disasters: a case study. *Energy Convers. Manag.* 221 (June), 113170. <https://doi.org/10.1016/j.enconman.2020.113170>.
- Arévalo, P., Jurado, F., 2020. Techno-economic evaluation of renewable energy systems combining PV-WT-HKT sources : effects of energy management under Ecuadorian conditions. *July*. <https://doi.org/10.1002/2050-7038.12567>.
- Atia, R., Yamada, N., 2012. Optimization of a PV-Wind-Diesel system using a hybrid genetic algorithm. *IEEE Electrical Power and Energy Conference* 80–85.
- Azam, A., Rafiq, M., Shafiq, M., Zhang, H., Ateeq, M., Yuan, J., 2021. Analyzing the relationship between economic growth and electricity consumption from renewable and non-renewable sources : fresh evidence from newly industrialized countries. *Sustain. Energy Technol. Assessments* 44 (September 2020), 100991. <https://doi.org/10.1016/j.seta.2021.100991>.
- Aziz, A.S., Faridun, M., Tajuddin, N., Adzman, M.R., Ramli, M.A.M., Mekhilef, S., 2019. Energy management and optimization of a PV/Diesel/Battery hybrid energy system using a combined dispatch strategy. *Sustainability* 11 (683), 1–26. <https://doi.org/10.3390/su11030683>.
- Aziz, A.S., Tajuddin, M.F.N., Zidane, T.E.K., Su, C.L., Alrubaie, A.J.K., Alwazzan, M.J., 2022. Techno-economic and environmental evaluation of PV/diesel/battery hybrid energy system using improved dispatch strategy. *Energy Rep.* 8, 6794–6814. <https://doi.org/10.1016/j.egypr.2022.05.021>.
- Babatunde, O.M., Adedoja, O.S., Babatunde, D.E., Denwigwe, I.H., 2019. Off-grid hybrid renewable energy system for rural healthcare centers: a case study in Nigeria. *Energy Sci. Eng.* 1–18. <https://doi.org/10.1002/ese3.314>.
- Bekele, Y., Biru, G., Bertling, L., 2023. ScienceDirect on the design and optimization of distributed energy resources for sustainable grid-integrated microgrid in Ethiopia. *Int. J. Hydrogen Energy*. <https://doi.org/10.1016/j.ijhydene.2023.04.192>.
- Chen, T., Wang, M., Babaei, R., Safa, M.E., Shojaei, A.A., 2023. Technoeconomic analysis and optimization of hybrid solar-wind-hydrodiesel renewable energy systems using two dispatch strategies. *Int. J. Photoenergy* 2023. <https://doi.org/10.1155/2023/3101876>.
- Dash, R.L., Mohanty, B., Hota, P.K., 2023. Energy , economic and environmental (3E) evaluation of a hybrid wind/biodiesel generator/tidal energy system using different energy storage devices for sustainable power supply to an Indian archipelago. *Renewable Energy Focus* 44, 357–372. <https://doi.org/10.1016/j.ref.2023.01.004>.
- Diyoke, C., Onyekachi, M., Okechukwu, T., 2023. Comparison of the grid and off-grid hybrid power systems for application in university buildings in Nigeria, 12 (2), 348–365.
- Gharibi, M., Askarzadeh, A., 2019. Size and power exchange optimization of a grid-connected diesel generator-photovoltaic-fuel cell hybrid energy system considering reliability , cost and renewability. *Int. J. Hydrogen Energy* 44 (47), 25428–25441. <https://doi.org/10.1016/j.ijhydene.2019.08.007>.
- Hossen, D., Islam, F., Ishraque, F., Shezan, S.A., Arifuzzaman, S.M., 2022. In: Design and implementation of a hybrid solar-wind-biomass renewable energy system considering meteorological conditions with the power system performances, p. 2022.
- Ishraque, F., Rahman, A., Shezan, S.A., 2022. In: Operation and assessment of a microgrid for Maldives: islanded and grid-tied mode, pp. 1–18.
- Ishraque, M.F., Shezan, S.A., Rana, M.S., Mueen, S.M., Rahman, A., Paul, L.C., Islam, M.S., 2021. Optimal sizing and assessment of a renewable rich standalone hybrid microgrid considering conventional dispatch methodologies. *Sustainability* 13 (22). <https://doi.org/10.3390/su132212734>.
- Jamshidi, S., Pourhossein, K., Asadi, M., 2021. Size estimation of wind/solar hybrid renewable energy systems without detailed wind and irradiation data : a feasibility study. *Energy Convers. Manag.* 234 (March), 113905. <https://doi.org/10.1016/j.enconman.2021.113905>.
- Jurado, F., Cano, A., Ar, P., 2020. Energy analysis and techno-economic assessment of a hybrid PV/HKT/BAT system using biomass gasifier: cuenca-Ecuador case study. <https://doi.org/10.1016/j.energy.2020.117727>.
- Kasaean, A., Rahdan, P., Amin, M., Rad, V., Yan, W., 2019. Optimal design and technical analysis of a grid-connected hybrid photovoltaic/diesel/biogas under different economic conditions: a case study. *Energy Convers. Manag.* 198 (July), 111810. <https://doi.org/10.1016/j.enconman.2019.111810>.
- Khiareddine, A., Ben Salah, C., Rekioua, D., Mimouni, M.F., 2018. Sizing methodology for hybrid photovoltaic/wind/hydrogen/battery integrated to energy management strategy for pumping system. *Energy* 153, 743–762. <https://doi.org/10.1016/j.energy.2018.04.073>.
- Lehtola, T., Zahedi, A., 2019. Solar energy and wind power supply supported by storage technology: a review. *Sustain. Energy Technol. Assessments* 35 (February), 25–31. <https://doi.org/10.1016/j.seta.2019.05.013>.
- Li, C., Zhou, D., Zhang, L., Shan, Y., 2022. Exploration on the feasibility of hybrid renewable energy generation in resource-based areas of China: case study of a regeneration city. *Energy Strategy Rev.* 42 (December 2021), 100869. <https://doi.org/10.1016/j.esr.2022.100869>.
- Malik, P., Awasthi, M., Sinha, S., 2020. Biomass-based gaseous fuel for hybrid renewable energy systems: an overview and future research opportunities. *August Int. J. Energy Res.* 1–31. <https://doi.org/10.1002/er.6061>.
- Mohamed, M.A., Eltamaly, A.M., Alolah, A.I., 2016. PSO-based smart grid application for sizing and optimization of hybrid renewable energy systems. *PLoS One* 11 (8), 1–22. <https://doi.org/10.1371/journal.pone.0159702>.
- Mousavi, S.A., Mehroooya, M., Amin, M., Rad, V., 2021. A new decision-making process by integration of exergy analysis and techno-economic optimization tool for the evaluation of hybrid renewable systems State of Charge. *Sustain. Energy Technol. Assessments* 45 (March), 101196. <https://doi.org/10.1016/j.seta.2021.101196>.
- NASA/SSE. (2016). Atmospheric Data Centre (2016) NASA Surface Meteorological and Solar Energy. <http://eosweb.larc.nasa.gov/sse>.
- NERC, 2005. Electric power sector Reform Act (EPSR), 2005. [https://nerc.gov.ng/index.php/library/documents/Regulations/Electric-Power-Sector-Reform-Act-\(EPSR\)-2005/](https://nerc.gov.ng/index.php/library/documents/Regulations/Electric-Power-Sector-Reform-Act-(EPSR)-2005/).
- Odou, O.D.T., Bhandari, R., Adamou, R., 2020. Hybrid off-grid renewable power system for sustainable rural electrification in Benin. *Renew. Energy* 145, 1266–1279. <https://doi.org/10.1016/j.renene.2019.06.032>.
- Oladigbolu, J.O., Ramli, M.A.M., Al-turki, Y.A., 2019. Techno-economic and sensitivity analyses for an optimal hybrid power system which is adaptable and Effective for rural electrification: a case study of Nigeria.
- Olatomiwa, L., Mekhilef, S., Ismail, M.S., Moghavvemi, M., 2016a. Energy management strategies in hybrid renewable energy systems : a review. *Renew. Sustain. Energy Rev.* 62, 821–835. <https://doi.org/10.1016/j.rser.2016.05.040>.

- Olatomiwa, L., Mekhilef, S., Ohunakin, O.S., 2016b. Hybrid renewable power supply for rural health clinics (RHC) in six geo-political zones of Nigeria. *Sustain. Energy Technol. Assessments* 13, 1–12. <https://doi.org/10.1016/j.seta.2015.11.001>.
- Olatomiwa, L., Sadiq, A.A., Longe, O.M., Ambafi, J.G., Jack, K.E., Abdulazeez, T.A., 2022. An overview of energy access solutions for rural healthcare facilities. *Energies* 12 (9554), 1–23. <https://doi.org/10.3390/en15249554>.
- PLAC, 2023. Electricity Act 2023. <https://placng.org/i/documents/electricity-act-2023/>.
- Ramesh, M., Saini, R.P., 2020. Dispatch strategies based performance analysis of a hybrid renewable energy system for a remote rural area in India. *J. Clean. Prod.* 259, 120697. <https://doi.org/10.1016/j.jclepro.2020.120697>.
- Ramesh, M., Saini, R.P., Ramesh, M., 2021. Environmental Effects Demand Side Management based techno- economic performance analysis for a stand-alone hybrid renewable energy system of India Demand Side Management based techno-economic performance analysis for a stand-alone hybrid renewable energy. *Energy Sources, Part A Recovery, Util. Environ. Eff.* 00 (00), 1–29. <https://doi.org/10.1080/15567036.2020.1851820>.
- Remteng, C., Suleiman, M.B., Asoegwu, C.M., Emenyonu, C.N., 2021. Nigeria electricity sector. [https://energypedia.info/wiki/Nigeria\\_Electricity\\_Sector#:~:text=The World Energy Outlook 2020 population estimated at 195 million](https://energypedia.info/wiki/Nigeria_Electricity_Sector#:~:text=The World Energy Outlook 2020 population estimated at 195 million).
- Shaaban, M., Petinrin, J.O., 2014. Renewable energy potentials in Nigeria: meeting rural energy needs. *Renew. Sustain. Energy Rev.* 29, 72–84. <https://doi.org/10.1016/j.rser.2013.08.078>.
- Shezan, S.A., Hasan, K.N., Rahman, A., Datta, M., Datta, U., 2021. In: Selection of appropriate dispatch strategies for effective planning and operation of a microgrid, pp. 1–19.
- Shezan, S.A., Ishraque, F., Muyeen, S.M., Abu-siada, A., Saidur, R., Ali, M.M., Rashid, M.M., 2022. Selection of the best dispatch strategy considering techno-economic and system stability analysis with optimal sizing. *Energy Strategy Rev.* 43 (August), 100923. <https://doi.org/10.1016/j.esr.2022.100923>.
- Shezan, S.A., Kamwa, I., Ishraque, M.F., Muyeen, S.M., Hasan, K.N., Saidur, R., Rizvi, S.M., Shafiullah, M., Al-Sulaiman, F.A., 2023. Evaluation of different optimization techniques and control strategies of hybrid microgrid: a review. *Energies* 16 (4), 1–30. <https://doi.org/10.3390/en16041792>.
- Suresh, V., Muralidhar, M., Kiranmayi, R., 2020. Modelling and optimization of an off-grid hybrid renewable energy system for electrification in a rural areas. *Energy Rep.* 6, 594–604. <https://doi.org/10.1016/j.egy.2020.01.013>.
- Toopshekan, A., Youse, H., Astaraei, F.R., 2020. Technical , economic , and performance analysis of a hybrid energy system using a novel dispatch strategy, 213. <https://doi.org/10.1016/j.energy.2020.118850>.
- Ugwoke, B., Gershon, O., Becchio, C., Corgnati, S.P., Leone, P., 2020. A review of Nigerian energy access studies : the story told so far. *Renew. Sustain. Energy Rev.* 120 (December 2019), 109646. <https://doi.org/10.1016/j.rser.2019.109646>.
- Uwineza, L., Kim, H.-G., Kleissl, J., Kim, C.K., 2021. Energy system. *Energies* 15 (2744), 573–573. [https://doi.org/10.1007/978-3-319-95864-4\\_300069](https://doi.org/10.1007/978-3-319-95864-4_300069).
- Yousef, B.A.A., Amjad, R., Ali, N., Rezk, H., 2022. Case Studies in Thermal Engineering Feasibility of integrated photovoltaic and mechanical storage systems for irrigation purposes in remote areas: optimization , energy management , and multicriteria decision-making. *Case Stud. Therm. Eng.* 38 (August), 102363. <https://doi.org/10.1016/j.csite.2022.102363>.